SUPPLEMENTAL MATERIAL

Wu et al. Novel microRNA regulators of atrial natriuretic peptide production

Supplementary Table 1. Summary of human atrial expression data, interaction with genetic variants, and luciferase assay data for the miRNAs predicted by at least 3 algorithms to target the *NPPA* 3'UTR. Evidence of expression (≥ 1000 sequence reads) in human atrial tissues were based on RNA sequencing data in Hsu *et al*.(1)

miRNA	Predicted by ≥ 3 algorithms to target *NPPA* 3'UTR?	Expressed ≥ 1000 reads in human atrial tissues (ref.(1))?	Seed binding site includes a genetic variant in the *NPPA* 3'UTR?	Reduces luciferase activity of WT-Luc construct ($p < 0.05$)?
miR-103a-3p	**Yes**	**Yes**	No	**Yes**
miR-105-5p	**Yes**	No	**Yes**	**Yes**
miR-107	**Yes**	**Yes**	No	**Yes**
miR-1184-1	**Yes**	No	No	Not tested
miR-1253	**Yes**	No	No	Not tested
miR-125a-3p	**Yes**	**Yes**	No	No
miR-1294	**Yes**	No	No	Not tested
miR-1301	**Yes**	No	No	Not tested
miR-136-5p	**Yes**	No	No	Not tested
miR-139-5p	**Yes**	**Yes**	No	No
miR-143-3p	**Yes**	**Yes**	No	No
miR-151a-5p	**Yes**	**Yes**	No	No
miR-155-5p	**Yes**	**Yes**	**Yes**	**Yes**
miR-183-5p	**Yes**	No	No	Not tested
miR-194-1	**Yes**	No	No	Not tested
miR-22-3p	**Yes**	**Yes**	No	No
miR-224-5p	**Yes**	No	No	Not tested
miR-24-3p	**Yes**	**Yes**	No	No
miR-342-5p	**Yes**	**Yes**	No	No
miR-425-5p	**Yes**	**Yes**	**Yes**	**Yes**

miR-497-3p	**Yes**	**Yes**	**Yes**	No
miR-498	**Yes**	No	No	Not tested
miR-508-5p	**Yes**	No	No	Not tested
miR-511	**Yes**	No	No	Not tested
miR-552	**Yes**	No	No	Not tested
miR-573	**Yes**	No	No	Not tested
miR-576-3p	**Yes**	No	No	Not tested
miR-582-5p	**Yes**	No	No	Not tested
miR-595	**Yes**	No	No	Not tested
miR-607	**Yes**	No	No	Not tested
miR-608	**Yes**	No	No	Not tested
miR-622	**Yes**	No	No	Not tested
miR-645	**Yes**	No	No	Not tested
miR-769-5p	**Yes**	**Yes**	**Yes**	No
miR-802	**Yes**	No	No	Not tested
miR-920	**Yes**	No	No	Not tested
miR-922	**Yes**	No	No	Not tested

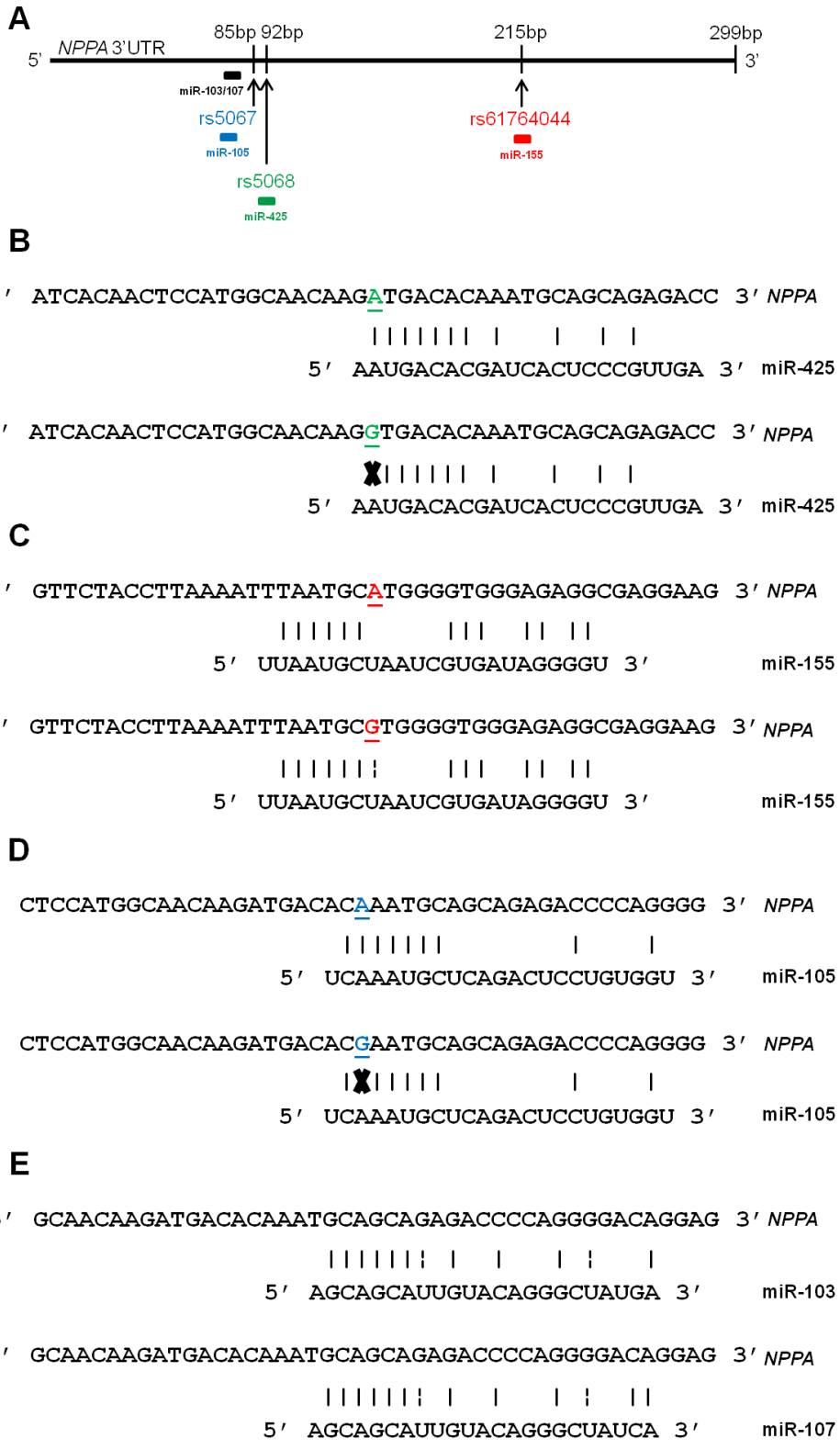

Supplementary Fig. S1. Schematic representation of the *NPPA* 3'UTR and the predicted alignment between miR-425, miR-155, miR-105, or miR-103/107 and *NPPA*.

(**A**) Diagram of the location of the genetic variants (rs5067, rs5068, and rs61764044) and the miRNA binding sites in the *NPPA* 3'UTR. (**B**) The position of rs5068 is shown in green. For the *NPPA* sequence, the sequence complementary to the *NPPA* mRNA is shown in the figure to highlight the alignment of miR-425 to sequences around the rs5068 DNA variant (2). The minor G allele of rs5068 disrupts the base pairing, as indicated by the X. (**C**) The position of rs61764044 is shown in red. For the *NPPA* sequence, the sequence complementary to the *NPPA* mRNA is shown in the figure to highlight the alignment of miR-155 to sequences around the rs61764044 DNA variant (2). The minor G allele of rs61764044 creates a G:U wobble base pairing, as indicated by the dashed line. (**D**) The position of rs5067 is shown in blue. For the *NPPA* sequence, the sequence complementary to the *NPPA* mRNA is shown in the figure to highlight the alignment of miR-105 to sequences around the rs5067 DNA variant (2). The minor G allele of rs5067 disrupts the base pairing, as indicated by the X. (**E**) For the *NPPA* sequence, the sequence complementary to the *NPPA* mRNA is shown in the figure. G:U wobble base pairing is indicated by the dashed line. miR-103 and miR-107 have the same sequence with the exception of the second to last nucleotide at the 3' end of the miRNA.

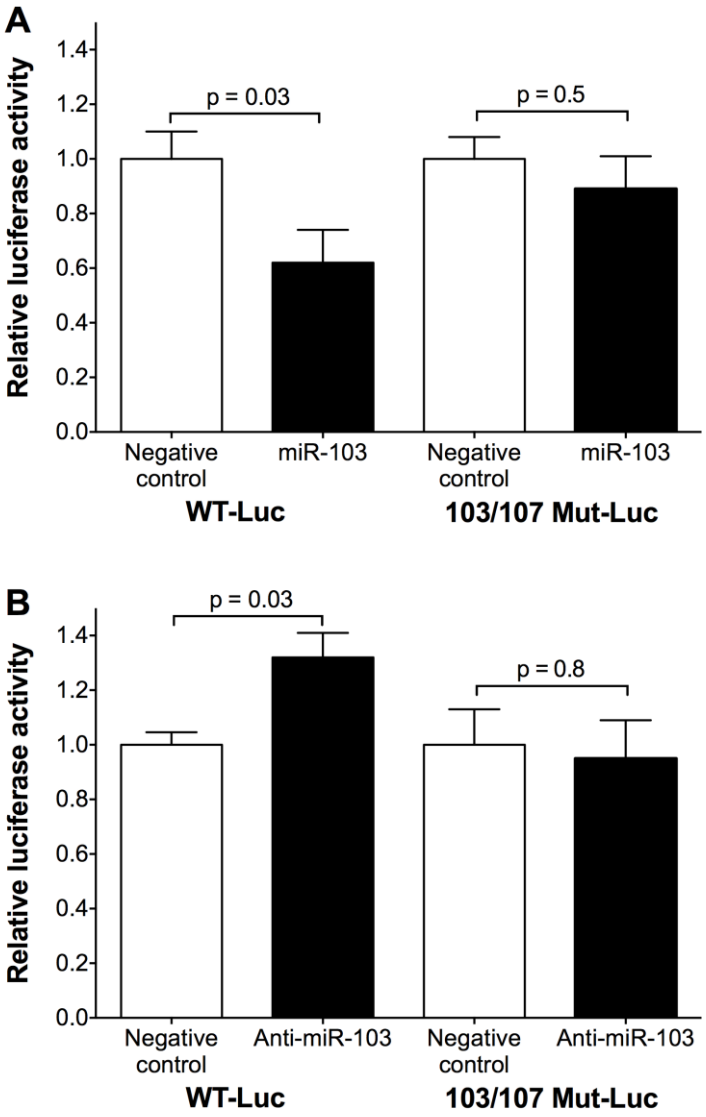

Supplementary Fig. S2. The *NPPA* 3'UTR is a direct target of miR-103. (**A**) miR-103 reduced the activity of the WT-Luc construct but not the 103/107 Mut-Luc construct with a 5-nucleotide mutation at the predicted miR-103/107 seed binding site. The ratio of firefly luciferase activity to renilla luciferase activity was normalized to the ratio in COS-7 cells transfected with constructs encoding luciferase without the *NPPA* 3'UTR and renilla. For each construct (WT-Luc or 103/107 Mut-Luc), the effect of the miRNA was compared to that of a scrambled negative control miRNA mimic (relative luciferase activity). (**B**) Anti-miR-103 increased the activity of the WT-Luc construct but not the 103/107 Mut-Luc construct. The ratio of firefly luciferase activity to renilla luciferase activity was normalized to the ratio in COS-7 cells transfected with constructs encoding luciferase without the *NPPA* 3'UTR and renilla. For each construct (WT-Luc or 103/107 Mut-Luc), the effect of the anti-miR was compared to that of a scrambled negative control anti-miR (relative luciferase activity). Data are mean ± SEM (n = 6 biological replicates), 2-tailed independent t test.

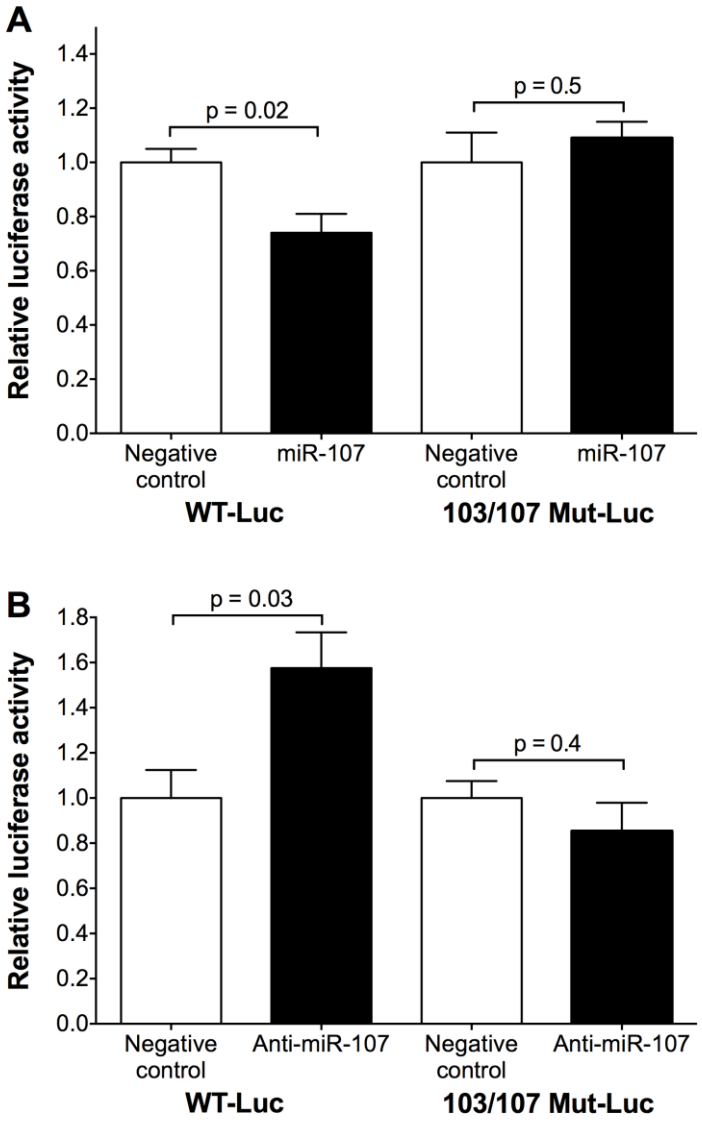

Supplementary Fig. S3. The *NPPA* 3'UTR is a direct target of miR-107. (**A**) miR-107 reduced the activity of the WT-Luc construct but not the 103/107 Mut-Luc construct with a 5-nucleotide mutation at the predicted miR-103/107 seed binding site. The ratio of firefly luciferase activity to renilla luciferase activity was normalized to the ratio in COS-7 cells transfected with constructs encoding luciferase without the *NPPA* 3'UTR and renilla. For each construct (WT-Luc or 103/107 Mut-Luc), the effect of the miRNA was compared to that of a scrambled negative control miRNA mimic (relative luciferase activity). (**B**) Anti-miR-107 increased the activity of the WT-Luc construct but not the 103/107 Mut-Luc construct. The ratio of firefly luciferase activity to renilla luciferase activity was normalized to the ratio in COS-7 cells transfected with constructs encoding luciferase without the *NPPA* 3'UTR and renilla. For each construct (WT-Luc or 103/107 Mut-Luc), the effect of the anti-miR was compared to that of a scrambled negative control anti-miR (relative luciferase activity). Data are mean ± SEM (n = 6 biological replicates), 2-tailed independent t test.

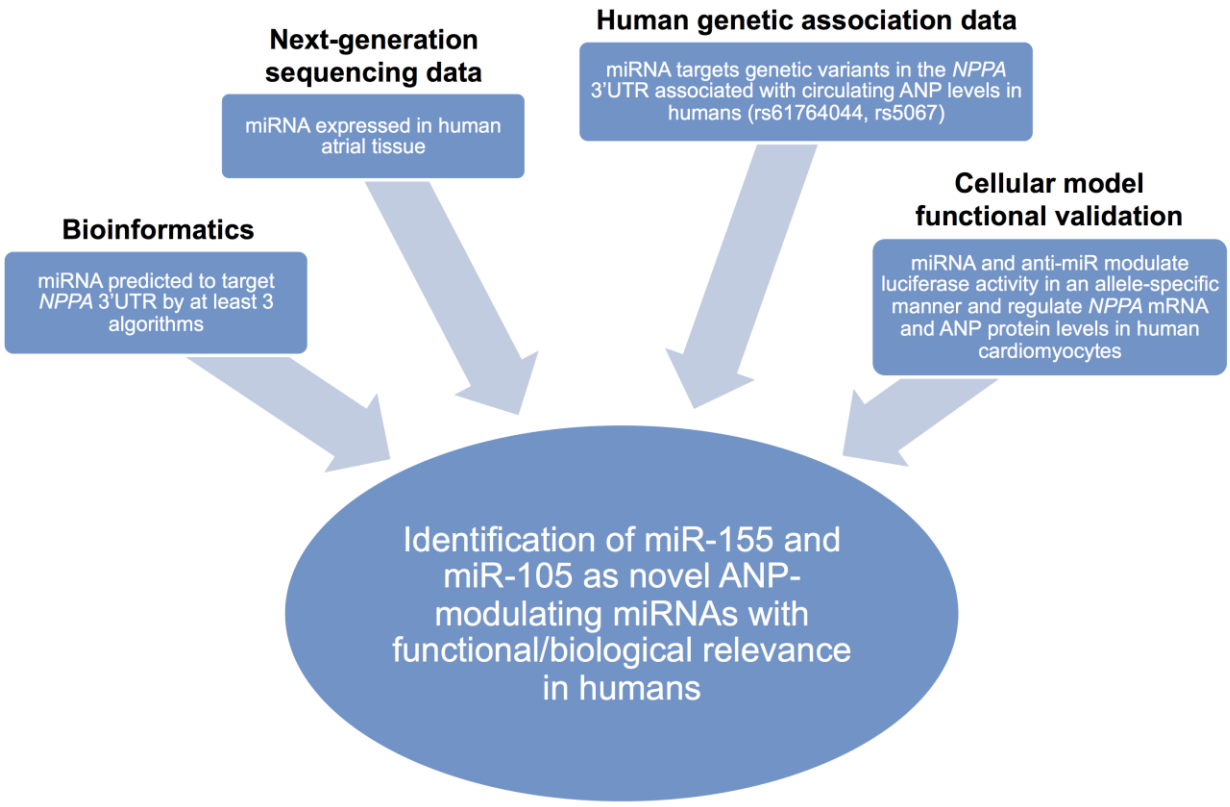

Supplementary Fig. S4. Illustration depicting the use of a multidimensional approach combining bioinformatics, next-generation sequencing data, human genetic association data, and cellular models to identify miR-155 and miR-105 as novel ANP-modulating miRNAs with functional/biological relevance in humans. Bioinformatics is used to identify miRNAs predicted to target the *NPPA* 3'UTR by at least 3 algorithms. Next-generation sequencing data is used to verify the expression of the miRNAs in human atrial tissues. Human genetic association data is used to highlight miRNAs (miR-155 and miR-105) that target genetic variants whose minor alleles are associated with higher circulating human ANP levels (rs61764044 and rs5067, respectively) and thus are likely to have biological relevance in regulating ANP levels in humans. Cellular models are used to validate the ability of the miRNAs to interact with *NPPA* mRNA in an allele-specific manner, with the minor allele of each respective variant conferring resistance to the miRNA, and modulate ANP production in human cardiomyocytes.

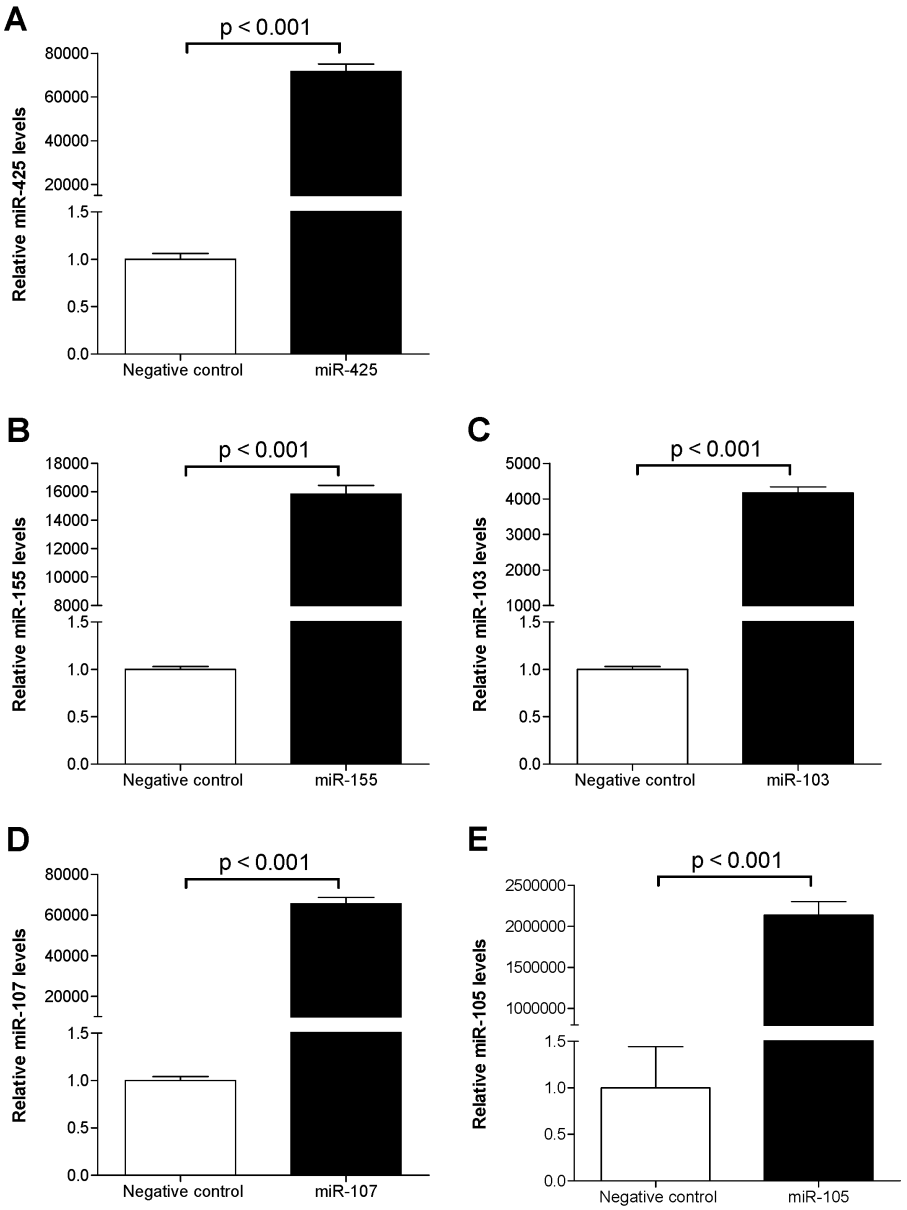

Supplementary Fig. S5. Levels of miRNA overexpression in COS-7 cells transfected with miRNA mimics. COS-7 cells were transfected with 5nM of miR-425, miR-155, miR-103, miR-107, miR-105, or a scrambled negative control miRNA mimic. Forty-eight hours later, cells were harvested, and miRNA expression levels were measured using qRT-PCR. (**A**) miR-425 levels in COS-7 cells transfected with miR-425 relative to cells transfected with negative control miRNA mimic. (**B**) miR-155 levels in COS-7 cells transfected with miR-155 relative to cells transfected with negative control miRNA mimic. (**C**) miR-103 levels in COS-7 cells transfected with miR-103 relative to cells transfected with negative control miRNA mimic. (**D**) miR-107 levels in COS-7 cells transfected with miR-107 relative to cells transfected with negative control miRNA mimic. (**E**) miR-105 levels in COS-7 cells transfected with miR-105 relative to cells transfected with negative control miRNA mimic. Data are mean ± SEM (n = 6 biological replicates), 2-tailed independent t test.

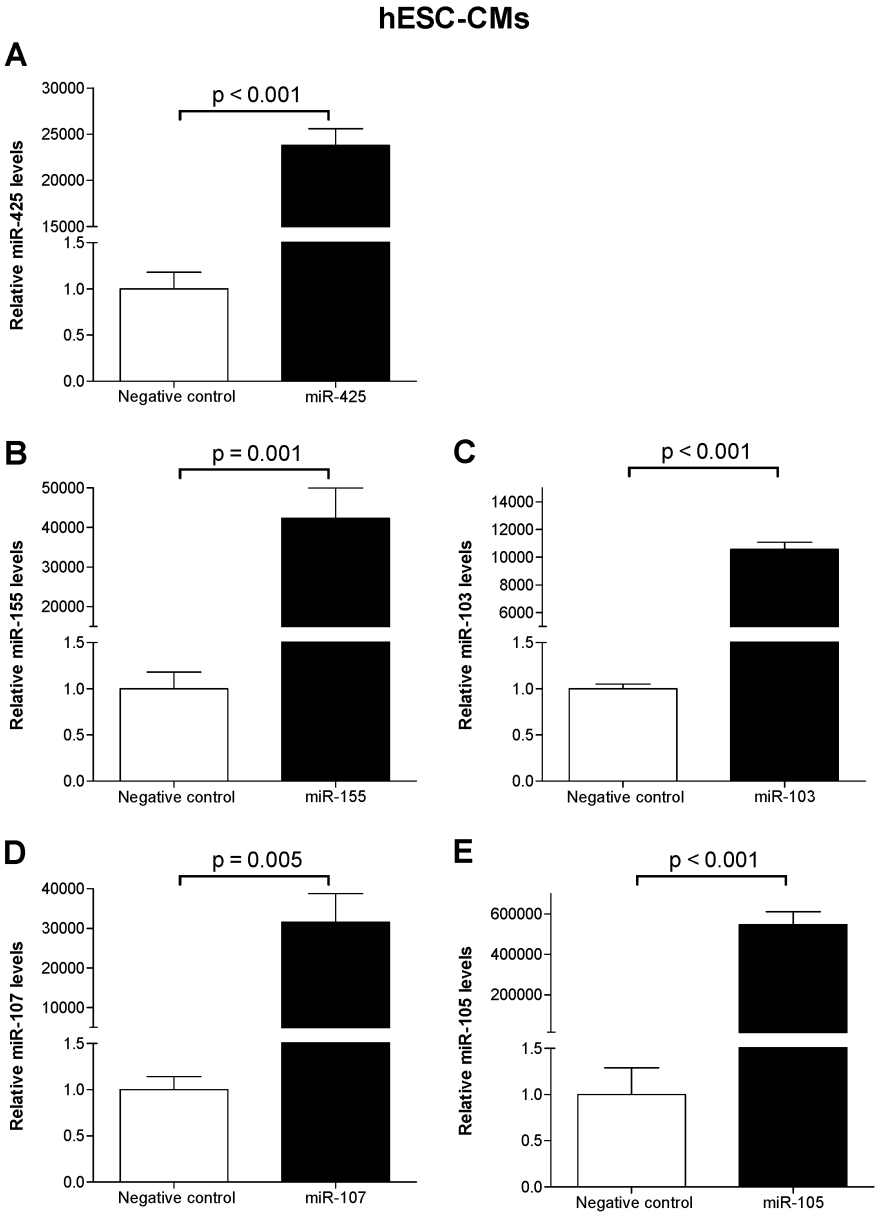

Supplementary Fig. S6. Levels of miRNA overexpression in hESC-CMs transfected with miRNA mimics. hESC-CMs (~1x10^5 per well) were transfected with 50nM of miR-425, miR-155, miR-103, miR-107, miR-105, or a scrambled negative control miRNA mimic. Twenty-four hours later, cells were washed and incubated in 1 mL of media. After an additional 24 hours, cells and media were harvested. miRNA expression levels were measured using qRT-PCR. (**A**) miR-425 levels in hESC-CMs transfected with miR-425 relative to cells transfected with negative control miRNA mimic. (**B**) miR-155 levels in hESC-CMs transfected with miR-155 relative to cells transfected with negative control miRNA mimic. (**C**) miR-103 levels in hESC-CMs transfected with miR-103 relative to cells transfected with negative control miRNA mimic. (**D**) miR-107 levels in hESC-CMs transfected with miR-107 relative to cells transfected with negative control miRNA mimic. (**E**) miR-105 levels in hESC-CMs transfected with miR-105 relative to

cells transfected with negative control miRNA mimic. Data are mean ± SEM (n = 6 biological replicates), 2-tailed independent t test.

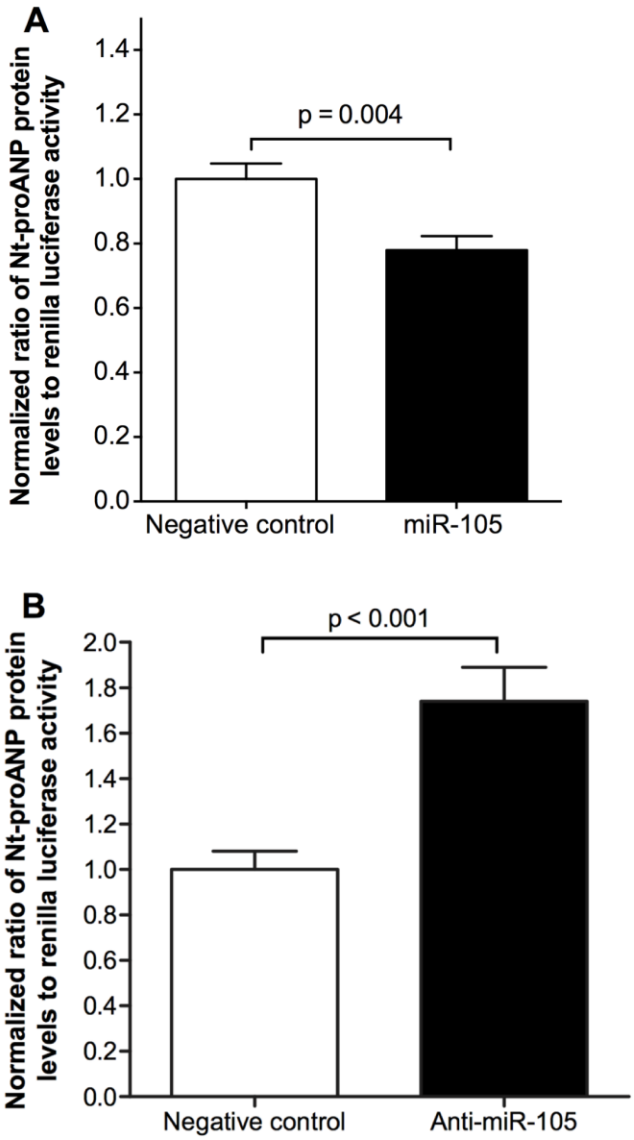

Supplementary Fig. S7. miR-105 suppresses and anti-miR-105 increases Nt-proANP production by heterologous cells transfected with a plasmid directing expression of a human *NPPA* cDNA. *NPPA* cDNA expression plasmid containing the rs5067 major allele was transfected into COS-7 cells together with a plasmid directing expression of renilla luciferase (as a control for transfection efficiency). Culture media was collected for measurement of secreted Nt-proANP protein levels (nmol/L), and cells were collected for measurement of renilla luciferase activity. (**A**) miR-105 reduced the secreted Nt-proANP protein levels relative to scrambled negative control miRNA mimic. (**B**) Anti-miR-105 increased the secreted Nt-proANP protein levels relative to scrambled negative control anti-miR. Data are expressed as the ratio of Nt-proANP protein levels measured in the culture medium normalized to the renilla luciferase activity (mean ± SEM; n=6 biological replicates, 2-tailed independent t test).

Supplementary References

1. **Hsu J, Hanna P, Van Wagoner DR, Barnard J, Serre D, Chung MK, Smith JD.** 2012. Whole genome expression differences in human left and right atria ascertained by RNA sequencing. Circ Cardiovasc Genet **5:**327-335.

2. **Barenboim M, Zoltick BJ, Guo Y, Weinberger DR.** 2010. MicroSNiPer: a web tool for prediction of SNP effects on putative microRNA targets. Hum Mutat **31:**1223-1232.